MicroRNA-31 predicts the presence of lymph node metastases and survival in lung adenocarcinoma patients

Wei Meng[1,4,#,] Zhenqing Ye[2,#], Ri Cui[3,4,5#], James Perry[1,4], Vaia Dedousi-Huebner[1], Alexander Huebner[1,4], Yao Wang[2], Bin Li[1,4], Stefano Volinia[3], Hiroshi Nakanishi[3,4], Taewan Kim[3,4], Sung-Suk Suh[3,4], Leona W. Ayers[6], Patrick Ross[7], Carlo M. Croce[3,4], Arnab Chakravarti[1], Victor X. Jin[2,$], Tim Lautenschlaeger[1$]

[1]Department of Radiation Oncology, The Ohio State University, Columbus, OH 43210;

[2]Department of Biomedical Informatics, The Ohio State University, Columbus, OH 43210

[3]Department of Molecular Virology, Immunology and Medical Genetics, The Ohio State University, Columbus, OH 43210

[4]Comprehensive Cancer Center, The Ohio State University, Columbus, OH 43210

[5]Yanbian University College of Medicine, Ji Lin, China

[6]Department of Pathology, College of Medicine, The Ohio State University, Columbus, OH, USA 43240

[7]Department of Surgery, Division of Thoracic Surgery, The Ohio State University, Columbus, OH, USA 43210

[#]Co-1st author

[$]Co-corresponding authors:

Dr. Tim Lautenschlaeger, Dept. of Radiation Oncology, Ohio State University, 400 W 12th Ave, 385G Wiseman Hall, Columbus, OH 43210. Tel: 614-2476432; email: TL@osumc.edu

Or Dr. Victor Jin, Dept. of Biomedical Informatics, 460 W 12th Ave., 212 BRT, Ohio State University, Columbus, OH 43210. Tel: (614) 292-6931; email: Victor.Jin@osumc.edu

The authors have no potential conflict of interest to disclose.

Running title: miRNA-31 in lung adenocarcinoma

Keywords: miRNA-seq, lung adenocarcinoma, metastasis, nodal stage, biomarker

Statement of Translational Relevance

SBRT is becoming a frequently performed treatment with curative intent for many patients with early stage NSCLC. Patients are typically staged with PET/CT to assess nodal involvement and surgical lymph node staging is rarely performed. However, PET sensitivity to identify cancerous lymph nodes is low for small nodes. We now present data suggesting that microRNA-31 increases invasiveness of lung adenocarcinoma resulting in more lymph node metastases, and worse outcome. Quantification of microRNAs in the primary lung tumor could be useful to estimate the likelihood of the presence of pathologically positive lymph nodes. MicroRNA-31 and other microRNAs therefore could be further developed as biomarkers to refine NSCLC patient selection for lung SBRT. Additionally, a better understanding of the degree of invasiveness of an individual tumor could guide the field of radiation oncology in the future to individualize radiation field expansions beyond the gross tumor to include invasive microscopic disease while maximizing normal tissue sparing.

Abstract

Purpose: We performed genome-wide microRNA-sequencing (miRNA-seq) in primary cancer tissue from lung adenocarcinoma patients to identify markers for the presence of lymph node metastasis.

Experimental Design: Markers for lymph node metastasis identified by sequencing were validated in a separate cohort using QPCR. After additional validation in the TCGA dataset, functional characterization studies were performed *in vitro*.

Results: MiR-31 was upregulated in lung adenocarcinoma tissues from patients with lymph node metastases compared to those without lymph node metastases. We confirmed miR-31 to be up-regulated in lymph node positive patients in a separate patient cohort ($p=0.009$, t-test), and to be expressed higher in adenocarcinoma tissue than in matched normal adjacent lung tissues ($p<0.0001$, paired t-test). MiR-31 was then validated as a marker for lymph node metastasis in an external validation cohort of 233 lung adenocarcinoma cases of the TCGA ($p=0.031$, t-test). *In vitro* functional assays showed that miR-31 increases cell migration, invasion, and proliferation in an ERK1/2 signaling dependent manner. Of note, miR-31 was a significant predictor of survival in a multivariate cox regression model even when controlling for cancer staging. Exploratory *in silico* analysis showed that low expression of miR-31 is associated with excellent survival for T2N0 patients.

Conclusions: We applied microRNA-seq to study microRNomes in lung adenocarcinoma tissue samples for the first time and identified potentially a microRNA predicting the presence of lymph node metastasis and survival outcomes in lung adenocarcinoma patients.

Introduction

Lung cancer is among the deadliest type of cancer in men and women. In 2012, there were an estimated 226,160 new cases of lung cancer and 160,340 deaths in the United States alone (1). Non small cell lung cancer (NSCLC) accounts for ~80% of all lung cancer patients and is further classified into subtypes, including adenocarcinoma (ADC), squamous cell carcinoma (SCC), and large cell lung carcinoma. Lung ADC is the most common lung cancer subtype comprising about 40% of all lung cancer patients. Survival has not improved significantly over several decades despite enormous research efforts.

MicroRNAs (miRNAs) are 20-22 nucleotide long, single-stranded non-coding RNAs, which regulate gene expression by transcriptional suppression (2). It is now well-known that microRNAs are involved in many different biological processes such as cell proliferation, cell death, and fat metabolism (3). Several studies have used microRNA expression profiling in primary tumors as a potential tool to identify novel signatures associated with diagnosis, staging, progression, prognosis as well as response to treatment (4, 5). The potential of microRNAs as prognostic or diagnostic biomarkers has been intensely evaluated and has shown great promise in certain cancer types, such as chronic lymphocytic leukemia (6), breast cancer (6), and lung cancer (7, 8). In lung ADC, one study reported that highly expressed pre-miR-155 and low expression of let-7 were correlated with poor prognosis (9). Another study identified miR-34a as a potential marker of relapse in surgically resected NSCLC (10), emphasizing the significance of microRNAs in NSCLC biology.

Recent advances in sequencing-based techniques allow the capture of a more complete set of transcription factor binding information, genomic interactions, high-resolution DNA methylation as well as mRNA transcripts in cells. The technique has further been used in studies to classify human cancers (11) and distinguish between induced pluripotent (iPS) and cancer stem cells (CSC) (12). However, most of these studies have been performed on *in vitro* cultured cell lines. Thus, we sought to apply this sequencing based approach to primary lung ADC tumor samples in order to identify novel associations between microRNAs and clinical variables including survival as well as to better understand the role of microRNAs in lung ADC pathobiology.

Lung ADC patients with mediastinal lymph node biopsy establishing early stage disease have been shown to be associated with lower local recurrence rates and improved overall survival (13). High dose radiation therapy using stereotactic ablative body radiation (SBAR) or stereotactic body radiation therapy (SBRT) in patients that are unfit for surgical treatment has been shown to be a successful approach (14). Currently, there are several ongoing clinical trials and several that are expected to soon report survival outcomes to evaluate the efficacy of SBRT for operable patients (i.e. ACOSOG Z4099/RTOG 1021, a phase III trial comparing sublobar resection with SBRT for high risk stage I NSCLC patients). SBRT is typically not preceded by surgical lymph node staging and patients routinely undergo PET/CT for staging. However, the sensitivity to detect metastatic tumor in lymph nodes smaller than 1cm on PET/CT is low (32.4% to 40% (15, 16). Molecular markers would thus be of great use as they would allow for a more accurate risk assesment of nodal metastasis in addition to PET scans, which ultimately could improve patient selection for SBRT beyond classical staging.

Additionally, a better understanding of the degree of invasiveness of an individual tumor could guide the field of radiation oncology in the future to individualize radiation field expansions beyond the gross tumor to include invasive microscopic disease and at the same time maximize normal tissue sparing. For these reasons we sought to identify molecular signatures of primary lung ADCs associated with the presence of lymph node metastases.

In this study we performed genome-wide microRNA-seq in lung ADC patient samples and used bioinformatic analyses to identify novel and annotated microRNAs that are differentially expressed between patients with and patients without lymph node metastasis, as well as examine their potential prognostic value. We selected one microRNA that was highly up-regulated in lung ADC patients with lymph node metastases for further characterization, including *in silico* mining of publicly available data generated by The Cancer Genome Atlas (TCGA) consortium and *in vitro* assays to characterize the function of this microRNA in lung ADC cell lines. Our study applied microRNA-seq for the first time to study microRNomes in lung ADC patient samples for the discovery of novel microRNA signatures that are potential biomarkers for outcomes in lung ADC.

Materials and Methods

Patients and tissue samples

Sixty four frozen tissue specimens from lung ADC patients collected between 2003 and 2012 were obtained through the OSUCCC Tissue Procurement Shared Resource

supported in part by the NCI Cancer Center Support Grant (CCSG-P30) and the Cooperative Human Tissue Network (CHTN/NCI), Midwestern Division, based on an internal review board (IRB) approved research protocol for this retrospective study. Other investigators may have received specimens from the same subjects. Remnant ADC tissues were flash frozen within two hours of surgical resection and stored at -80^{o}C until analysis. Samples were received with a coded final pathology report and a quality assessment report verifying collection of tumor and/or normal adjacent tissue.

microRNA extraction

MicroRNA samples from fresh frozen tissue were extracted using PureLink™ microRNA Isolation Kit (Life Technologies Corporation, Carlsbad, CA). Briefly, 5 mg fresh frozen tissue samples were mixed with 300 µl Binding Buffer (L3) and homogenized using a tissue homogenizer. Homogenized samples were centrifuged, and the supernatants were mixed with 300 µl 70% ethanol. Solutions containing RNA were purified by two rounds of spin column cleanup and RNA was eluted with 50 µl sterile RNase-free water.

microRNA-seq

Total RNA samples were processed by the flashPAGE fractionator (Ambion) and flashPAGE Clean-Up Kit (Ambion). Enriched small RNA was then processed according to the SOLiD Small RNA Expression Kit protocol (Applied Biosystems) and purified small RNAs were ligated with 5' and 3' adapter Mix using RNA ligase. Ligated products (40–60 bases in length) were reverse transcribed and purified on Novex 10% TBE-Urea gel. Subsequently, 15–18 cycles of PCR were performed by amplifying the purified

cDNA with barcoded PCR primer sets provided with the kit, which differed by a unique 6-nucleotide sequence. Amplified products were loaded on Novex 6% TBE gel (Invitrogen) and the gel bands containing 110 to 130bp fragments were excised. Amplified products were purified from the excised gel band and then loaded on the Applied Biosystems SOLiD next generation high throughput sequencing system for data acquisition. The quality of the samples and libraries were verified on the Agilent Bioanalyzer (17).

RT-qPCR

To validate the identified targets from SOLiD system, quantitative real-time (qRT) PCR was used on fresh frozen tissue samples. The miR-31 (miR-31-5p) and the small nuclear RNA U6 were analyzed in triplicates by TaqMan MicroRNA Assay kits (Applied Biosystems, Darmstadt, Germany). A 30ng sample of RNA was processed by the TaqMan MicroRNA Reverse Transcription kit (Applied Biosystems, Darmstadt, Germany). In brief, 5 µl RNA was mixed with 1 mmol/l of each deoxyribonucleotide triphosphate, 50 units of Multiscribe Reverse Transcriptase, 5 × reaction buffers, 4 units RNase inhibitor, and 5× gene-specific RT primers mix in a final reaction volume of 15 µl. Reactions were then incubated at 16°C for 30 min, 42°C for 30 min, 85°C for 15 min with a final hold at 4°C.

Afterward, 15 µl of the cDNA solution was diluted by nuclease-free water to a final volume of 100 µl. Quantitive PCR was run on a 7900 HT PCR machine with denaturation step at 95°C for 10 minutes, followed by 40 cycles of a denaturation step at 95°C for 15 seconds, and an annealing/elongation step at 60°C for 60 seconds. Fold change for

microRNA in tissue samples was then calculated using the equation 2-ΔCt test / 2- ΔCt control. Paired student t-test was performed to identify if miR-31 is differentially expressed between cancer and matched normal adjacent tissues ($p<=0.05$). Welch's t-test was performed to test if miR-31 expression is different between patients with and without lymph node metastasis to account for unequal variances. For sensitivity and specificity analysis receiver operator characteristic (ROC) as well as area under the curve (AUC) was determined using CART (Classification and Regression Trees).

microRNA-seq data analysis

Among the total 64 tissue samples, 10 samples (6 with N0 stage and 4 with N1+ stage) were sequenced using the SOLiD platform. First, all reads were trimmed by removing the 3' adaptor sequence using the Cutadapt program (18), and the length distribution of reads for each sample has been plotted (Supplementary Figure 1). Subsequently, we used a "Sequential Trim Alignment (SeqTrimAlign)" strategy to map all reads to the hg19 reference genome in color space (19), in which the last one color base of those unmapped reads in the previous alignment round would be trimmed, and re-submited to the next round of alignment using Bowtie (20), until a minimum read length was reached, in our case 19 color bases. This strategy is believed to fit specifically for solid data and could promote a high mapping ratio without sacrificing much performance. Detection of novel microRNAs was performed by miRDeep2 using the above alignment, which utilizes the position and frequency of reads uniquely aligned to the genome ("signature") with respect to a putative RNA hairpin and scores the microRNA candidate employing a probabilistic model based on microRNA biogenesis (17). The more positive the score the

more reliable the prediction would be. We chose predicted microRNAs as novel candidates if they had a score >= 2.0 and were present in at least 3 samples. Applying these selection criteria 65 novel microRNAs were identified in our data set, that were then included in the following expression analysis.

Expression analysis of microRNA-Seq data was performed using the R/Bioconductor package EdgeR (21), which is designed for use with digital gene expression data. First, we counted the number of reads uniquely mapped to microRNA regions according to the reference database miRBase (22) and novel microRNAs identified as above; then the normalization and differential expression between the N0 group and N1+ group was assessed in EdgeR by calculating an exact test p-value analogous to the Fisher's exact test.

Target prediction was performed for miR-31, which was identified to be expressed higher in ADC N1+ patients than in N0 patients. Currently, there is no single bioinformatics tool with accurate microRNA target prediction. However, integration of various computational methods is a common approach to improve prediction accuracy and to create an optimal framework for deciphering biological functions of microRNAs. We used the miRWalk database (23) which reports predicted microRNA-mRNA interactions on the 3' UTRs of known genes calculated by several established target prediction programs including TargetScan (24), miRanda (25) and RNAhybrid (26). Statistically significant microRNA-mRNA relationships were extracted from the results using two criteria: p-value <= 0.05 and identification by at least five of the six selected target prediction programs.

TCGA dataset

The TCGA microRNA-seq data set with clinical information was downloaded on 07/18/2012. The set included 341 level 3 lung ADC microRNA data sets. 233 out of the 341 patients from the TCGA lung ADC cohort had outcome as well as staging information available and were non-metastatic. Those 233 cases were used for correlative analysis. For analysis of the TCGA data set Welch's t-test was performed to test if miR-31 expression is different between patients with and without lymph node metastasis to account for unequal variances.

To assess if miR-31 controls the EMT program we performed correlative analysis of miR-31 expression and genes known to be up or down regulated during EMT (27). A total of 174 lung adenocarcinoma samples containing both gene expression and miR-31 expression were extracted from the 233 patient set with available microRNA expression data. Since only level 3 data was analyzed, no additional normalization was performed. Correlation coefficients were calculated using log2(EMT gene expression) and log2(miR-31 expression) data. The zero miR-31 expression values or EMT gene expression values were replaced by the minimum non-zero expression value of miR-31 or EMT gene.

Study of dependency between miR-31 expression levels and miR-31 promoter methylation status was analyzed using Illumina Infinium Human DNA Methylation 450 beadchip data. A total of 177 lung adenocarcinoma samples containing both methylation and miR-31 expression were extracted from the 233 patient set. Spearman correlation coefficient was calculated using beta-values of methylation probe cg05146756 (Chromosome 9: 21548871) and log2(microRNA31 expression). The zero miR-31

expression values or methylation beta-values were replaced by the minimum non-zero expression value of miR-31 or beta-values of cg05146756 probe.

Survival analysis

233 out of a total of 341 patients from the TCGA lung ADC cohort had clinical information available and were used for correlative analysis. TCGA cohort staging was performed according to either AJCC 6th edition or 7th edition, and tumor size was not available. The decision to classify Mx patients as M0 for the purpose of this study was made on the clinical experience that pathologic synoptic reports commonly report Mx for clinically non-metastatic tumor patients and that surgical primary tumor removal is typically only performed in those patients. MiR-31 expression was log2 transformed to construct normal distribution. The associations between overall survival of all patients with the expression levels of miR-31, as well as the survival of T2N0 patients with the expression level of miR-31 were analyzed by using the Kaplan-Meier method, log-rank test, and Cox proportional hazard regression models. Statistical significance was accepted for $P < 0.05$.

Graphs were generated with GraphPad Prism 5 for windows.

IPA for pathway enrichment analysis

Analysis of biological functions of target genes by miR-31 was performed using the Ingenuity Pathways Analysis software. Target genes of miR-31 were uploaded to IPA to identify relevant cellular and metabolic functions and molecular networks. Pathways with $P < 0.015$ were determined to be significant and were included in further analysis.

Cell lines and regents

Human lung ADC cell lines H23, H1573, and H2228, were purchased from the American Type Culture Collection (ATCC) and passaged for less than six months in RPMI1640 medium containing 10% fetal bovine serum (FBS). ATCC authenticates its cell lines using short tandem repeat (STR) profiling. The antibodies against Actin-beta, Vimentin, Twist and SNAI1 were purchased from Santa Cruz Biotechnology (Santa Cruz, CA, USA). Antibodies against phospo-AKT, AKT, phospho-ERK1/2, ERK1/2, and Actin were purchased from Cell Signaling Technology (Danvers, MA, USA). Cells were pre-incubated with 10 uM AZD6244 from AstraZeneca (Wilmington, DE, USA) for 24 hours before performing the assays as outlines below.

Infection of H23, H1573, and H2228 cells with the lentiviral miR-31 expression and/or miRZip-31 anti-miR-31 constructs

H23, H1573, and H2228 cells were stably infected with the human pre-microRNA expression construct Lenti-miR-31 vector and human miRZip-31 anti-miR-31 microRNA construct, respectively (System biosciences). The empty vectors were used as a control. The pre-miR-31, miRZip-31 anti-miR-31 and control constructs were packaged with pPACKH1 Lentivector Packaging Plasmid mix (System Biosciences) in a 293TN packaging cell line. The Transdux reagent (System Bioscience) was used for virus transduction and infected cells were selected by FACS analysis (FACSCalibular, BD Bioscience).

Cell migration and invasion assays

In vitro cell migration and invasion assay were performed using Boyden chambers (BD bioscience) that use 8 μm micropore membranes without Matrigel (for migration assay) or with Matrigel (for invasion assay). Both assays were carried out according to the manufacturer's instructions. The cells were resuspended in 0.1% BSA in RPMI1640 medium and seeded in the upper chamber at a concentration of 5×10^4/500μl. The chambers were incubated in the wells containing RPMI1640 medium with 10% FBS for 24 or 48 hours. Filters were fixed with 5% glutaraldehyde and stained with 1% crystal violet. The cells on the upper surface of the filters were removed by swabbing with a cotton swab and the cells that had migrated to the reverse side were counted in 10 random fields under a microscope at ×100 or ×200 magnification.

***In vitro* cell growth rates**

Cultured cells were placed into 24-well plates at 2×10^4 cells/well in triplicate. After 3 days, the numbers of cells were quantified using a Cell Counting Kit 8 (Dojindo, Kumamoto, Japan) as described previously (28).

Western blot analysis

The cells were lysed with RIPA buffer containing Protease/Phosphatase Inhibitor Cocktail (Cell Signaling Technology, Danvers, MA) and 10 or 50 μg protein lysates per lane were separated on 4-20% SDS-PAGE and then electrotransferred to nitrocellulose or PVDF membranes. Membranes were blocked with blocking solution (1 or 5% bovine serum albumin in TBST) and incubated with primary antibody in 3% bovine serum

albumin in TBST, followed by incubation with appropriate HRP-conjugated secondary antibody. Specific proteins were detected using the enhanced chemiluminescence system (GE Healthcare).

Results

Identification of a microRNA signature associated with the presence of lymph node metastasis

We selected 43 cases with 64 tissue specimens available from lung ADC patients (Supplementary table 1) and performed genome-wide microRNA-seq on tissues from 10 cases (Table 1 , and analysis flow chart Supplementary Figure 2). In four of those 10 cases lymphnode metastasis was present (pN1 and pN2, referred to as N1+) and in six cases mediastinal lymphnode dissection was performed but no lymph node metastasis was identified (pN0). Using the EdgeR program (21) with a fold change cutoff of 2 and a p-value less than 0.05, we identified 32 annotated and three novel microRNAs that were differentially expressed between the N1+ and N0 groups. Of 35 differentially expressed miRs, 29 were up-regulated in N1+ cases and six were down-regulated (Supplementary Figure 3). Among these, miR-9, miR-31, miR-34 family and miR-224 have been previously reported to be deregulated in human cancers (29-32). Interestingly, we found that miR-31was up-regulated in N1+ patients in our study cohort (Figure 1A) consistent with miR-31 previously reported to be up-regulated in metastatic colon cancer (33) but contrary to the reported high expression of miR-31 associated with reduced frequency of metastases in breast cancer (34).

We then performed RT-qPCR of miR-31, which has not yet been reported to be associated with lymph node or distant metastasis in lung ADCs, on the original 10 patients' specimens as well as on an additional 54 tissue specimens (clinical information of patients in Supplementary Table 1). There was good concordance between miR-31-5p qPCR (delta Ct) and miR seq (RPM normalized reads) data with a Pearson correlation coefficient of 0.554 (n=10). Consistent with previous reports (35), miR-31 expression was higher in lung ADC cancer tissues compared to their matched normal adjacent tissues (paired t-test p=2.86E-5, n=21, Figure 1B). Comparing miR expression by qPCR in a validation cohort of cancer tissues from patients with lymph node metastasis (N1+, n=10) and patients without lymph node metastasis (N0, n=23) there was a higher expression of miR-31 in N1+ patients than N0 patients (4.23 fold increase in N1+ patients, p=0.009) (Figure 1C). Sensitivity/specificity analysis revealed a receiver operator characteristic area under the curve of AUC=0.79 in the combined set (cohorts 1 + 2, n=43) (Supplementary Figure 4).

We then tested our miR-31 lung ADC lymph node metastasis signature in an external validation set. The publicly available TCGA miR seq data set with limited clinical information was downloaded on 07/18/2012. Of the evaluable 249 patients with staging and survival information available, 140 patients had N0M0 disease, 93 patients had positive lymph nodes but no distant metastasis (N1+ M0), and 16 patients had distant metastasis (M1) (clinical information of 233 M0 patients in Supplementary Table 2). Among the 93 cases of the N1+M0 patient group 49 patients had N1 disease, 43 patients had N2 disease, and one patient had N3 disease. MiR-31 was 2.5 fold up-regulated in primary lung ADC patients with lymph node metastasis (N1+M0) compared to those

without (N0M0) (t-test p=0.031 Figure 1D). The 16 patients with M1 disease showed a statistically non-significant, but numerically higher expression of miR-31 compared to M0 patients. Similar results were obtained if the 43 patients with prior cancer diagnosis were excluded from the analysis (2.96 fold, t-test p=0.02 for miR-31 for N0M0 vs N1+M0 comparison).

Prognostic value of miR-31

After establishing that miR-31 is associated with the presence of lymph node metastasis and given the knowledge that lymph node metastasis is a well established prognostic factor, we examined the prognostic value of miR-31 in the publicly available TCGA data set. Factors associated with increased hazard of death on univariate analysis included miR-31 expression (log-rank test p =8.50E-04), N stage (log-rank test p = 1.27E-4 for N1 stage, p= 2.59E-6 for N2+ stage), and T3 stage (log-rank test p = 1.61E-03).

To formally evaluate if miR-31 expression is significantly associated with survival independent from lymph node involvement, we performed Cox proportional hazards modeling on 233 lung ADC cases. In a multivariate Cox proportional hazard regression model including miR-31 expression, age, sex, lymph node stage, tumor stage, race, prior cancer diagnosis, and smoking history, the following factors were significant predictors of survival: miR-31 expression, nodal stage, and prior cancer diagnosis (Table 2).

After understanding that miR-31 expression is of prognostic value in lung ADC, independent of lymph node status, we performed an exploratory correlative analysis of miR-31 in the T2N0 patient subset given the controversy related to possible benefits of adjuvant chemotherapy in those patients and the need for novel biomarkers in this patient

group (36, 37). We found that high miR-31 expression is associated with adverse outcome in T2N0 lung ADC patients (log-rank p=0.0194), and remarkably there was no death observed for almost two years in the group with low miR-31 expression in the TCGA cohort (Supplementary Figure 5).

In silico targets of miR-31 signature

Many studies have shown that downstream targets of microRNAs often regulate cancer initiation and progression (38, 39). Therefore, we wanted to further examine the targets of miR-31 and the pathways those targets are involved in to better understand the function of this microRNA. We applied the TargetScan software designed for *in silico* prediction of microRNA targets to identify the targets of miR-31. We found that 143 genes are predicted to be regulated by miR-31 when requiring prediction by at least five of the six selected target prediction algorithms using a p-value cutoff of 0.05. We performed IPA analysis on the set of miR-31 targets and found that the top five canonical pathways for miR-31 targeted genes are CDK5, PTEN, p70S6K, ERK/MAPK and PI3K /AKT signaling (Supplementary Figure 6). The top five categories of associated biological functions are cell death and survival, cell cycle, cell morphology, cellular growth and proliferation, cellular function and maintenance (Supplementary Table 3).

Functional validation of miR-31 in lung cancer cell lines

As described above, miR-31 was significantly upregulated in lung ADC patients with lymph node metastasis (N1+M0) compared to those without (N0M0). In order to functionally characterize miR-31, we tested migration, invasion and proliferation in three

lung ADC cell lines (H23, H2228, and H1573) (Supplementary Table 4). H23 and H2228 cells were transduced with a Lenti-miR vector containing miR-31 precursor to overexpress miR-31 in this cell line. H1573 cells were transduced with a vector containing a miRZip-31 anti-miR-31 microRNA construct to knockdown miR-31. The expression levels of miR-31, following treatment, were confirmed by qRT-PCR (Figure 2A, Supplementary Figure 7A, and Supplementary Figure 8A). In response to overexpression of miR-31, cell invasion into Matrigel-coated transwell membranes was markedly increased (Figure 2B and Supplementary Figure 7B). Overexpression of miR-31 also significantly increased migratory and proliferative ability of H23 and H2228 cells (Figure 2C, Figure 2D, Supplementary Figure 7C and Supplementary Figure 7D). Conversely, knockdown of miR-31 in H1573 cells significantly reduced cell invasion (Supplementary Figure 8B), migration (Supplementary Figure 8C), and proliferation (Supplementary Figure 8D). We then tested if the *in silico* identified miR-31 targeted pathways were indeed altered in our cell culture models. Pathway analysis identified ERK/MAPK and PI3K/AKT signaling as two of the top pathways related to genes that are predicted targets of miR-31. Identified pathways were analyzed for changes in activation by western blot after miR-31 overexpression or knockdown. We observed no major signaling alterations in PI3K/AKT, however we observed a reduction in ERK1/2 signaling in our H1573 miR-31 knockdown cell line and an increase in ERK1/2 activation in our H23 and H2228 miR-31 overexpression cell lines (Figure 3A, 3B and 3C). To test if ERK1/2 signaling is necessary for miR-31 to induce an invasive phenotype we assessed proliferation and migration in the H23 and H2228 cell lines overexpressing miR-31 after treatment with the MEK inhibitor AZD6244 (10 uM). ERK1/2 signaling

inhibition indeed suppressed the previously observed increases in profliferation or migration in miR-31 overexpressing cell lines compared to control cells (Figure 4A, 4B, and 4C; Supplementary Figure 9A, 9B and 9C), suggesting that ERK1/2 pathway activation is a main mediator of the miR-31 induced invasive phenotype. ERK1/2 is known to be an important regulator of proliferation and migration (40). This observed association of miR-31 expression and ERK pathway activation is consistent with our observed phenotype in migration, invasion and proliferation in miR-31 knockdown and overexpression cells. We then tested if the association between miR-31 expression and ERK phosphorylation can also be observed in tissue samples. There was no correlation identified (data not shown). To explore possible reasons for this observation we assessed if miR-31 expression levels are similar in cell lines and in the tissues profiled (Supplementary Figure 10). MiR-31 expression levels were overall lower in tissues than in cell lines, which might contribute to the observed lack of correlation of pERK and miR-31 in tissues.

Epithelial/mesenchymal transition (EMT) has been reported as a key process in tumor invasion, metastasis and tumorigenicity. Several EMT-activating markers including Vimentin (*VIM*), *ZEB1*, *SNAI1*, and *TWIST1* have been identified to be involved in this process (27, 41). We investigated the relationship between expression of these EMT-related markers and miR-31 expression in our lung ADC cell lines. As shown in Supplementary Figure 11, the expression of Vimentin, TWIST1 and SNAI1 were increased after overexpression of miR-31 in H23 cells. A difference in expression in those proteins was not observed in H1573 miR-31 knockdown cells (data not shown). Given these observations we sought out to systematically assess if miR-31 could be a

regulator of EMT. To this end we analyzed associations of miR-31 expression and genes known to be up regulated or down regulated during EMT using the TCGA data set (Supplementary table 5). Of note, the three EMT markers Vimentin, TWIST1 and SNAI1, which had been shown to be upregulated in the H23 miR-31 overexpressing cell line also were positively correlated in the TCGA dataset. Overall there were numerous EMT markers significantly correlated with miR-31 expression, indicating that miR-31 might contribute to the control of EMT. It remains to be determined if ERK signaling activation and EMT are co-incident events or if one leads to the other. However, we present data indicating that ERK signaling is necessary for the miR-31 induced invasive phenotype.

MiR-31 expression is controlled by promoter methylation

To understand if miR-31 is controlled by promoter methylation the TCGA dataset was examined for correlation of miR-31 promoter methylation and miR-31 expression. There was a strong anti-correlation (correlation coefficient = -0.61, p=4.4e-13), which suggests that DNA promoter methylation leads to repressed miR-31 expression.

Discussion

In this study, we applied microRNA-seq, a next generation sequencing (NGS) technique, to identify microRNAs associated with lymph node metastasis in lung ADC patient tissue samples. We identified and validated miR-31 to be associated with the presence of lymph node metastasis and patient survival. We further showed that miR-31 modulates the migratory, invasive and proliferative behavior of lung ADC cell lines in culture.

Among the 32 annotated and 3 novel microRNAs identified with our comprehensive approach, there were several microRNAs such as miR-9, miR-31, the miR-34 family and miR-224 that have been previously reported to be deregulated in human cancers (29-32). MiR-31 was previously reported to be upregulated in colon cancer tissues compared to benign tissues and was shown to increase proliferation and migration in intestinal cell lines (42), suggesting that miR-31 could be associated with tumor progression and have pro-metastasis functions. In squamous cell cancer of lung, high expression of miR-31 was associated with poor patient survival (43). In our study, we found miR-31 to be upregulated in lung ADC tissues from patients that have lymph node metastasis of adenocarcinoma, and further show *in vitro* that miR-31 leads to ERK1/2 pathway activation and promotes migration, invasion and proliferation (44). While we show that ERK signaling is necessary for the miR-31 mediated invasive phenotype and while there is evidence that ERK signaling can promote EMT (45, 46), it remains to be determined if miR-31 mediated ERK signaling activation and EMT are coincident events or if one leads to another. High expression of miR-31 in breast differs and has been reported to be associated with reduced frequency of metastasis (34). MiR-31 likely suppresses metastasis in breast cancer by targeting the metastasis-promoting genes ITGA5, RDX and RhoA (47), and over-expression of miR-31 in established breast cancer metastases can lead to regression of those metastases (48). In prostate cancer high levels of miR-31 are associated with better outcomes (49, 50). Previously it has been shown that miR-31 has tumorigenic effects in lung cancer cell lines via repression LATS2 and PPP2R2A, genes with known tumor-suppressive function (35). In smooth muscle cells miR-31 expression appears to be controlled by ERK1/2 signaling and lead to LATS2 degradation mediated

increase in proliferation (51). However, a more recent report suggests DICER1, also a gene with known tumor-suppressive function, and not LATS2 or PPP2R2A is the functionally relevant miR-31 target in lung squamous cell carcinoma (43). These findings suggest that miR-31 is playing an important role in tumor progression and metastasis formation in multiple cancers. However, the function of mir-31 appears to depend on the genetic background of the tumor.

We initially sought out to identify novel markers of lymph node metastasis. Given the increased use and success of SBRT for early stage lung cancer and the low sensitivity of PET/CT for the detection of tumor positive small lymph nodes (<1cm), markers to more accurately assess the risk of nodal involvement beyond imaging studies are very useful. We identified miR-31, a microRNA known to be deregulated in many cancers, to be upregulated in lung ADCs of patients with involved lymph nodes. MicroRNAs appear to have potential for further development as markers to assess the risk of lymph node involvement using primary tumor biopsy tissues. Furthermore, we demonstrated that miR-31 is an independent prognostic marker for lung ADC even when controlling for known prognostic factors such as tumor stage.

Given the controversy over T2N0 lung ADC patients and possible benefits from adjuvant chemotherapy (36, 47, 52), we performed an exploratory survival analysis of T2N0 patients in the TCGA data set to assess if the miR-31 signature for lymph node metastasis is of prognostic value in this patient subpopulation. We found that high miR-31 expression is associated with adverse outcome in T2N0 lung ADC patients, and remarkably there were no deaths observed for nearly two years in the low miR-31

expression group in the TCGA cohort. However, given that the TCGA data at this time includes only 70 death events (about 30% of included cases) this observation needs to be interpreted with caution. Our findings if validated may provide a rationale to evaluate microRNAs as biomarkers to determine which T2N0 patients might benefit from additional cancer therapy.

In summary, our findings have several implications: 1. MicroRNA-seq of tumor tissue is a feasible approach for biomarker discovery 2. MicroRNAs could predict not only the presence of lymph node metastasis but also clinical outcome 3. The mechanisms of how miR-31 controls invasion and metastasis appear to be complex and context specific as miR-31 plays a pro-metastatic role in lung adenocarcinoma, and lung squamous cell carcinoma, but plays an anti-metastatic role in breast cancer and is a good prognostic marker in prostate cancer.

Acknowledgement

This work was supported by the Department of Radiation Oncology (T.L), the Comprehensive Cancer Center (A.C.), and the Department of Biomedical Informatics (V.X.J), The Ohio State University. The OSUCCC Tissue Procurement Shared Resource is supported in part by the Ohio State University NCI Cancer Center Support Grant (CCSG-P30). The project described was supported by Award Number Grant 8UL1TR000090-05 from the National Center For Advancing Translational Sciences. The content is solely the responsibility of the authors and does not necessarily represent the official views of the National Center For Advancing Translational Sciences or the National Institutes of Health.

References

1. Siegel R, Naishadham D, Jemal A. Cancer statistics, 2012. CA Cancer J Clin. 2012;62:10-29.

2. Lagos-Quintana M, Rauhut R, Lendeckel W, Tuschl T. Identification of novel genes coding for small expressed RNAs. Science. 2001;294:853-8.

3. Ambros V. MicroRNA pathways in flies and worms: growth, death, fat, stress, and timing. Cell. 2003;113:673-6.

4. Lu J, Getz G, Miska EA, Alvarez-Saavedra E, Lamb J, Peck D, et al. MicroRNA expression profiles classify human cancers. Nature. 2005;435:834-8.

5. Lu Y, Govindan R, Wang L, Liu PY, Goodgame B, Wen W, et al. MicroRNA profiling and prediction of recurrence/relapse-free survival in stage I lung cancer. Carcinogenesis. 2012;33:1046-54.

6. Calin GA, Ferracin M, Cimmino A, Di Leva G, Shimizu M, Wojcik SE, et al. A MicroRNA signature associated with prognosis and progression in chronic lymphocytic leukemia. The New England journal of medicine. 2005;353:1793-801.

7. Yu SL, Chen HY, Chang GC, Chen CY, Chen HW, Singh S, et al. MicroRNA signature predicts survival and relapse in lung cancer. Cancer cell. 2008;13:48-57.

8. Yanaihara N, Caplen N, Bowman E, Seike M, Kumamoto K, Yi M, et al. Unique microRNA molecular profiles in lung cancer diagnosis and prognosis. Cancer cell. 2006;9:189-98.

9. Takamizawa J, Konishi H, Yanagisawa K, Tomida S, Osada H, Endoh H, et al. Reduced expression of the let-7 microRNAs in human lung cancers in association with shortened postoperative survival. Cancer research. 2004;64:3753-6.

10. Gallardo E NA, Vinolas N, Marrades RM, Diaz T, et al. miR-34a as a prognostic marker of relapse in surgically resected non-small-cell lung cancer. Carcinogenesis. 2009:1903–9.

11. Comprehensive molecular characterization of human colon and rectal cancer. Nature. 2012;487:330-7.

12. Bissels U, Wild S, Tomiuk S, Hafner M, Scheel H, Mihailovic A, et al. Combined characterization of microRNA and mRNA profiles delineates early differentiation pathways of CD133+ and CD34+ hematopoietic stem and progenitor cells. Stem Cells. 2011;29:847-57.

13. Sarwate D, Sarkar S, Krimsky WS, Burgan CM, Patel K, Evans R, et al. Optimization of mediastinal staging in potential candidates for stereotactic radiosurgery of the chest. The Journal of thoracic and cardiovascular surgery. 2012;144:81-6.

14. Timmerman R, Paulus R, Galvin J, Michalski J, Straube W, Bradley J, et al. Stereotactic body radiation therapy for inoperable early stage lung cancer. JAMA : the journal of the American Medical Association. 2010;303:1070-6.

15. Bille A, Pelosi E, Skanjeti A, Arena V, Errico L, Borasio P, et al. Preoperative intrathoracic lymph node staging in patients with non-small-cell lung cancer: accuracy of integrated positron emission tomography and computed tomography. European journal of cardio-thoracic surgery : official journal of the European Association for Cardio-thoracic Surgery. 2009;36:440-5.

16. Al-Sarraf N, Gately K, Lucey J, Wilson L, McGovern E, Young V. Lymph node staging by means of positron emission tomography is less accurate in non-small cell lung cancer patients with enlarged lymph nodes: analysis of 1,145 lymph nodes. Lung Cancer. 2008;60:62-8.

17. Friedlander MR, Chen W, Adamidi C, Maaskola J, Einspanier R, Knespel S, et al. Discovering microRNAs from deep sequencing data using miRDeep. Nature biotechnology. 2008;26:407-15.

18. Martin M. Cutadapt removes adapter sequences from high-throughput sequencing reads. EMBnetjournal, North America. 2011.

19. Marco A, Griffiths-Jones S. Detection of microRNAs in color space. Bioinformatics. 2012;28:318-23.

20. Langmead B, Salzberg SL. Fast gapped-read alignment with Bowtie 2. Nature methods. 2012;9:357-9.

21. Robinson MD, McCarthy DJ, Smyth GK. edgeR: a Bioconductor package for differential expression analysis of digital gene expression data. Bioinformatics. 2010;26:139-40.

22. Griffiths-Jones S, Grocock RJ, van Dongen S, Bateman A, Enright AJ. miRBase: microRNA sequences, targets and gene nomenclature. Nucleic acids research. 2006;34:D140-4.

23. Dweep H, Sticht C, Pandey P, Gretz N. miRWalk--database: prediction of possible miRNA binding sites by "walking" the genes of three genomes. Journal of biomedical informatics. 2011;44:839-47.

24. Lewis BP, Shih IH, Jones-Rhoades MW, Bartel DP, Burge CB. Prediction of mammalian microRNA targets. Cell. 2003;115:787-98.

25. John B, Enright AJ, Aravin A, Tuschl T, Sander C, Marks DS. Human MicroRNA targets. PLoS biology. 2004;2:e363.

26. Kruger J, Rehmsmeier M. RNAhybrid: microRNA target prediction easy, fast and flexible. Nucleic acids research. 2006;34:W451-4.

27. Roy S, Chakravarty D, Cortez V, De Mukhopadhyay K, Bandyopadhyay A, Ahn JM, et al. Significance of PELP1 in ER-negative breast cancer metastasis. Mol Cancer Res. 2012;10:25-33.

28. Cui R, Takahashi F, Ohashi R, Yoshioka M, Gu T, Tajima K, et al. Osteopontin is involved in the formation of malignant pleural effusion in lung cancer. Lung Cancer. 2009;63:368-74.

29. Ma L, Young J, Prabhala H, Pan E, Mestdagh P, Muth D, et al. miR-9, a MYC/MYCN-activated microRNA, regulates E-cadherin and cancer metastasis. Nature cell biology. 2010;12:247-56.

30. Valastyan S, Weinberg RA. miR-31: a crucial overseer of tumor metastasis and other emerging roles. Cell Cycle. 2010;9:2124-9.

31. Choi YJ, Lin CP, Ho JJ, He X, Okada N, Bu P, et al. miR-34 miRNAs provide a barrier for somatic cell reprogramming. Nature cell biology. 2011;13:1353-60.

32. Li Q, Wang G, Shan JL, Yang ZX, Wang HZ, Feng J, et al. MicroRNA-224 is upregulated in HepG2 cells and involved in cellular migration and invasion. Journal of gastroenterology and hepatology. 2010;25:164-71.

33. Cekaite L, Rantala JK, Bruun J, Guriby M, Agesen TH, Danielsen SA, et al. MiR-9, -31, and -182 Deregulation Promote Proliferation and Tumor Cell Survival in Colon Cancer. Neoplasia. 2012;14:868-81.

34. Valastyan S, Reinhardt F, Benaich N, Calogrias D, Szasz AM, Wang ZC, et al. A pleiotropically acting microRNA, miR-31, inhibits breast cancer metastasis. Cell. 2009;137:1032-46.

35. Liu X, Sempere LF, Ouyang H, Memoli VA, Andrew AS, Luo Y, et al. MicroRNA-31 functions as an oncogenic microRNA in mouse and human lung cancer cells by repressing specific tumor suppressors. The Journal of clinical investigation. 2010;120:1298-309.

36. Strauss GM, Herndon JE, 2nd, Maddaus MA, Johnstone DW, Johnson EA, Harpole DH, et al. Adjuvant paclitaxel plus carboplatin compared with observation in stage IB non-small-cell lung cancer: CALGB 9633 with the Cancer and Leukemia Group B, Radiation Therapy Oncology Group, and North Central Cancer Treatment Group Study Groups. Journal of clinical oncology : official journal of the American Society of Clinical Oncology. 2008;26:5043-51.

37. Katz A, Saad ED. CALGB 9633: an underpowered trial with a methodologically questionable conclusion. Journal of clinical oncology : official journal of the American Society of Clinical Oncology. 2009;27:2300-1; author reply 1-2.

38. Li Z, Yang CS, Nakashima K, Rana TM. Small RNA-mediated regulation of iPS cell generation. The EMBO journal. 2011;30:823-34.

39. Hanina SA, Mifsud W, Down TA, Hayashi K, O'Carroll D, Lao K, et al. Genome-wide identification of targets and function of individual MicroRNAs in mouse embryonic stem cells. PLoS genetics. 2010;6:e1001163.

40. Dhillon AS, Hagan S, Rath O, Kolch W. MAP kinase signalling pathways in cancer. Oncogene. 2007;26:3279-90.

41. Yang J, Weinberg RA. Epithelial-mesenchymal transition: at the crossroads of development and tumor metastasis. Dev Cell. 2008;14:818-29.

42. Cottonham CL, Kaneko S, Xu L. miR-21 and miR-31 converge on TIAM1 to regulate migration and invasion of colon carcinoma cells. The Journal of biological chemistry. 2010;285:35293-302.

43. Tan X, Qin W, Zhang L, Hang J, Li B, Zhang C, et al. A 5-microRNA signature for lung squamous cell carcinoma diagnosis and hsa-miR-31 for prognosis. Clinical cancer research : an official journal of the American Association for Cancer Research. 2011;17:6802-11.

44. Lautenschlaeger T, Meng W, Ye Z, Cui R, Perry J, Huebner A, et al. Lung adenocarcinoma microRNA-31 expression levels to predict lymph node metastasis and patient survival. Journal of clinical oncology : official journal of the American Society of Clinical Oncology. 2013;31:suppl; abstr 7573.

45. Shin S, Dimitri CA, Yoon SO, Dowdle W, Blenis J. ERK2 but not ERK1 induces epithelial-to-mesenchymal transformation via DEF motif-dependent signaling events. Mol Cell. 2010;38:114-27.

46. Ha GH, Park JS, Breuer EK. TACC3 promotes epithelial-mesenchymal transition (EMT) through the activation of PI3K/Akt and ERK signaling pathways. Cancer Lett. 2013;332:63-73.

47. Valastyan S, Chang A, Benaich N, Reinhardt F, Weinberg RA. Concurrent suppression of integrin alpha5, radixin, and RhoA phenocopies the effects of miR-31 on metastasis. Cancer research. 2010;70:5147-54.

48. Valastyan S, Chang A, Benaich N, Reinhardt F, Weinberg RA. Activation of miR-31 function in already-established metastases elicits metastatic regression. Genes & development. 2011;25:646-59.

49. Xu RS, Wu XD, Zhang SQ, Li CF, Yang L, Li DD, et al. The tumor suppressor gene RhoBTB1 is a novel target of miR-31 in human colon cancer. Int J Oncol. 2012.

50. Lin PC, Chiu YL, Banerjee S, Park K, Mosquera JM, Giannopoulou E, et al. Epigenetic repression of miR-31 disrupts androgen receptor homeostasis and contributes to prostate cancer progression. Cancer research. 2013;73:1232-44.

51. Liu X, Cheng Y, Chen X, Yang J, Xu L, Zhang C. MicroRNA-31 regulated by the extracellular regulated kinase is involved in vascular smooth muscle cell growth via large tumor suppressor homolog 2. The Journal of biological chemistry. 2011;286:42371-80.

52. Butts CA, Ding K, Seymour L, Twumasi-Ankrah P, Graham B, Gandara D, et al. Randomized phase III trial of vinorelbine plus cisplatin compared with observation in completely resected stage IB and II non-small-cell lung cancer: updated survival analysis of JBR-10. Journal of clinical oncology : official journal of the American Society of Clinical Oncology. 2010;28:29-34.

Patient	Lymph Node Stage	Age	Sex	Tumor Stage	No. of Total Reads	No. of Unique Reads	Smoking History	Mutation Status		
								EGFR	KRAS	ALK
1	0	53	F	2	9960689	5713626	Current reformed smoker for < or = 15 years (50 packs/year)	N/A	N/A	N/A
2	0	79	F	2	12515046	7662059	Current smoker (45 pack-years)	N/A	N/A	N/A
3	0	62	F	2	5976179	3572120	Lifelong non-smoker	N/A	N/A	N/A
4	0	58	M	2	15558403	7180012	Current smoker (40 pack-years)	N/A	N/A	N/A
5	0	65	F	2	11203103	6029716	Current reformed smoker for < or = 15 years (50 pack-years)	positive	N/A	N/A
6	0	69	F	1	20995778	9497072	History of smoking but current status unknown (90 pack-years)	N/A	N/A	N/A
7	1	61	F	1	5800498	3115660	N/A	N/A	N/A	N/A
8	2	81	M	2	15154937	10401873	N/A	N/A	N/A	N/A
9	2	66	F	2	20576378	9869855	Current smoker	N/A	N/A	N/A
10	2	68	M	2	9486218	5164859	History of smoking but current status unknown	N/A	N/A	N/A

Table 1. A summary of clinical and miRNA-seq information for 10 lung ADC patients

Characteristic	No. of patients	Hazard Ratio	%95 CI	P	
miR-31	233	1.14	1.04 to 1.26	6.47E-03	**
Age at diagnosis	233	1.01	0.98 to 1.04	0.56	
Sex					
Female	127	1	reference		
Male	106	0.89	0.48 to 1.62	0.69	
N stage					
0	140	1	reference		
1	49	3.51	1.84 to 6.72	1.47E-04	***
2+	44	4.56	2.24 to 9.27	2.75E-05	***
T stage					
1	70	1	reference		
2	132	1.04	0.52 to 2.09	0.92	
3	21	1.62	0.52 to 5.09	0.41	
4	10	1.62	0.48 to 5.51	0.44	
Prior cancer diagnosis					
No	191	1	reference		
YES	42	2.77	1.45 to 5.29	2.10E-03	**
Race					
White	186	1	reference		
African	15	1.16	0.37 to 3.6	0.80	
Asian	3	NA	NA	NA	
NA	29	0.91	0.37 to 2.24	0.83	
Smoking					
Lifelong Non-smoker	27	1	reference		
Current reformed smoker for > 15 years	58	1.00	0.38 to 2.64	1.00	
Current reformed smoker for < or = 15 years	82	1.24	0.51 to 3.01	0.64	
Current smoker	53	0.72	0.27 to 1.93	0.51	
NA	13	0.75	0.248 to 2.24	0.60	

Significance. codes: $P \leq 0.001$ '***', $P \leq 0.01$ '**', $P \leq 0.05$ '*', ns ' '

Table 2. Multivariate Cox proportional hazards model

Figure Legends

Figure 1. microRNA deep sequencing reveals miR-31 expression is higher in primary lung adenocarcinoma tissue from patients with lymph node metastasis (N1+) than without (N0). **B** miR-31 expression in 21 pairs of matched normal adjacent tissues and lung ADC tissues (paired t-test, p=2.86 E-5). **C** miR-31 expression in an independent cohort of 23 N0 vs. 10 N1+ lung ADC patients (t-test, p=0.009). **D** miR-31 expression in 140 N0 patients vs. 93 N1+ patients from the TCGA lung ADC dataset (t-test, p=0.031). The middle bar represents the mean, upper and lower border of the box represents 25th and 75th percentiles, and the whiskers go down to the 5th percentile and up to the 95th percentile.

Figure 2. Ectopic expression of miR-31 increases migration/invasion capabilities of H23 cells. (A) Expression of miR-31 following infection with Lenti-miR vector containing miR-31 precursor was confirmed by TaqMan real-time PCR. (B) Cell invasion assay for miR-31 overexpressing H23 cells. (C) Cell migration assay for miR-31 overexpressing H23 cells using transwell membranes (upper panel, representative pictures of migration chambers; bottom panel, average counts from 10 random microscopic fields). The average counts were derived from ten random microscopic fields. (D) Cell proliferation assay for miR-31 knockdown H23 cells. Data are presented as mean ± S.D. *P<0.05.

Figure 3. (A) Reduction in ERK1/2 signaling in the H1573 miR-31 knockdown cell line. (B) ERK1/2 signaling activation in the H23 miR-31 overexpression cell line. (C) ERK1/2 signaling activation in the H2228 miR-31 overexpression cell line.

Figure 4. The effect of MEK inhibitor, AZD6244, on miR31 induced cell proliferation and migration. (A) pERK1/2 expression in H23/miR31 cells after treatment with AZD6244. Cell proliferation (B) and migration (C) assay for miR31 overexpressing H23 and control cells after treatment with AZD6244.

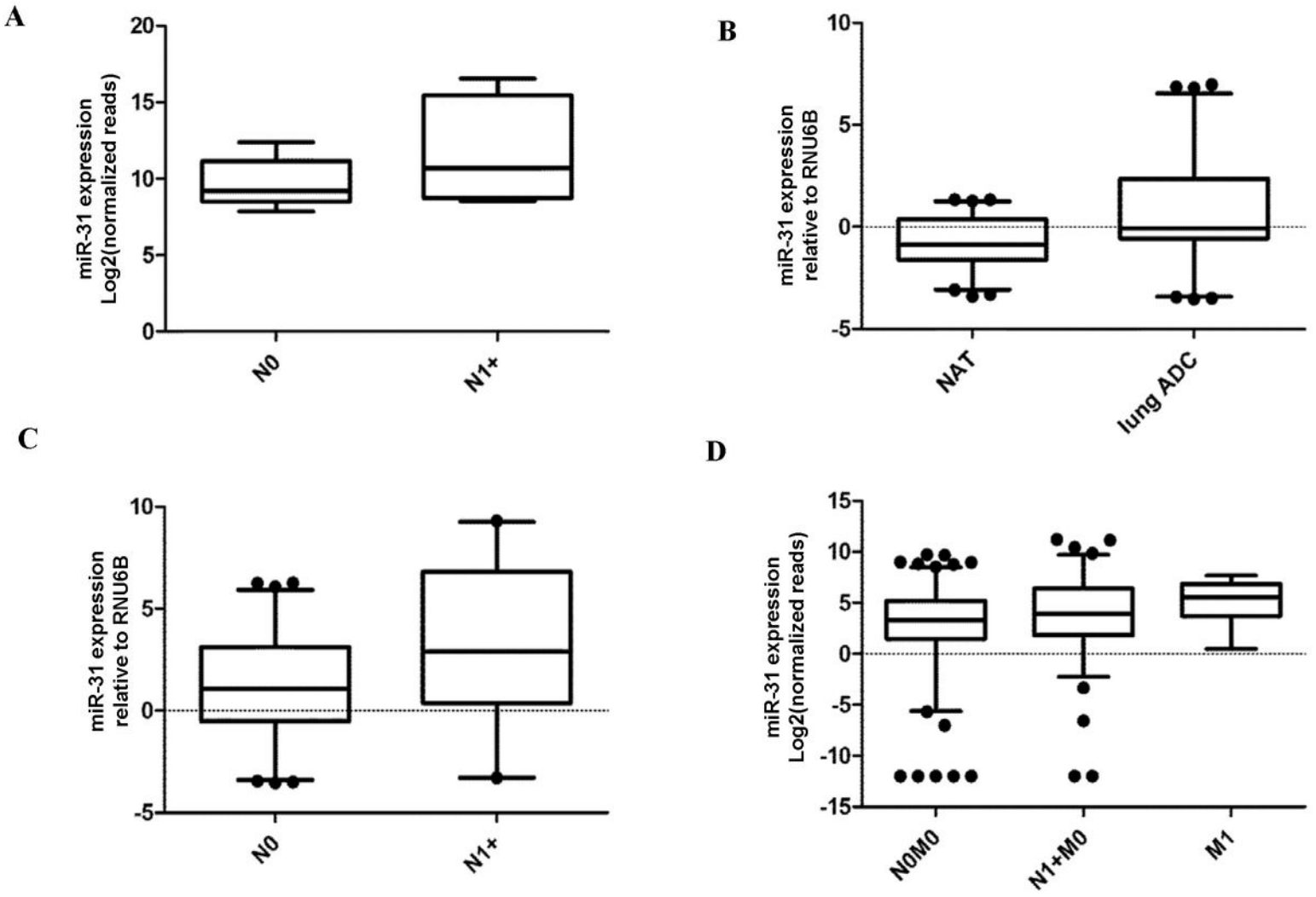

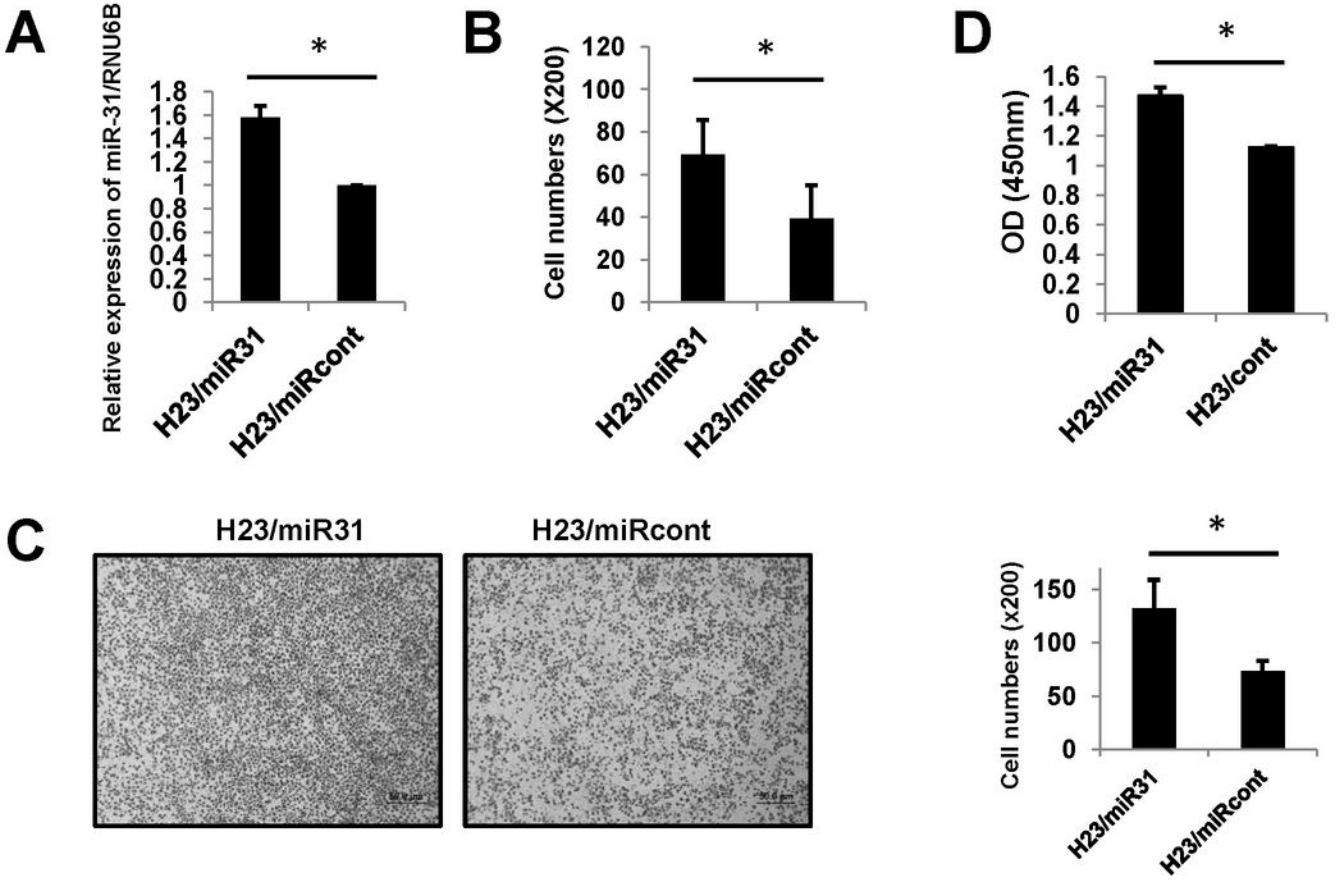

Figure 3

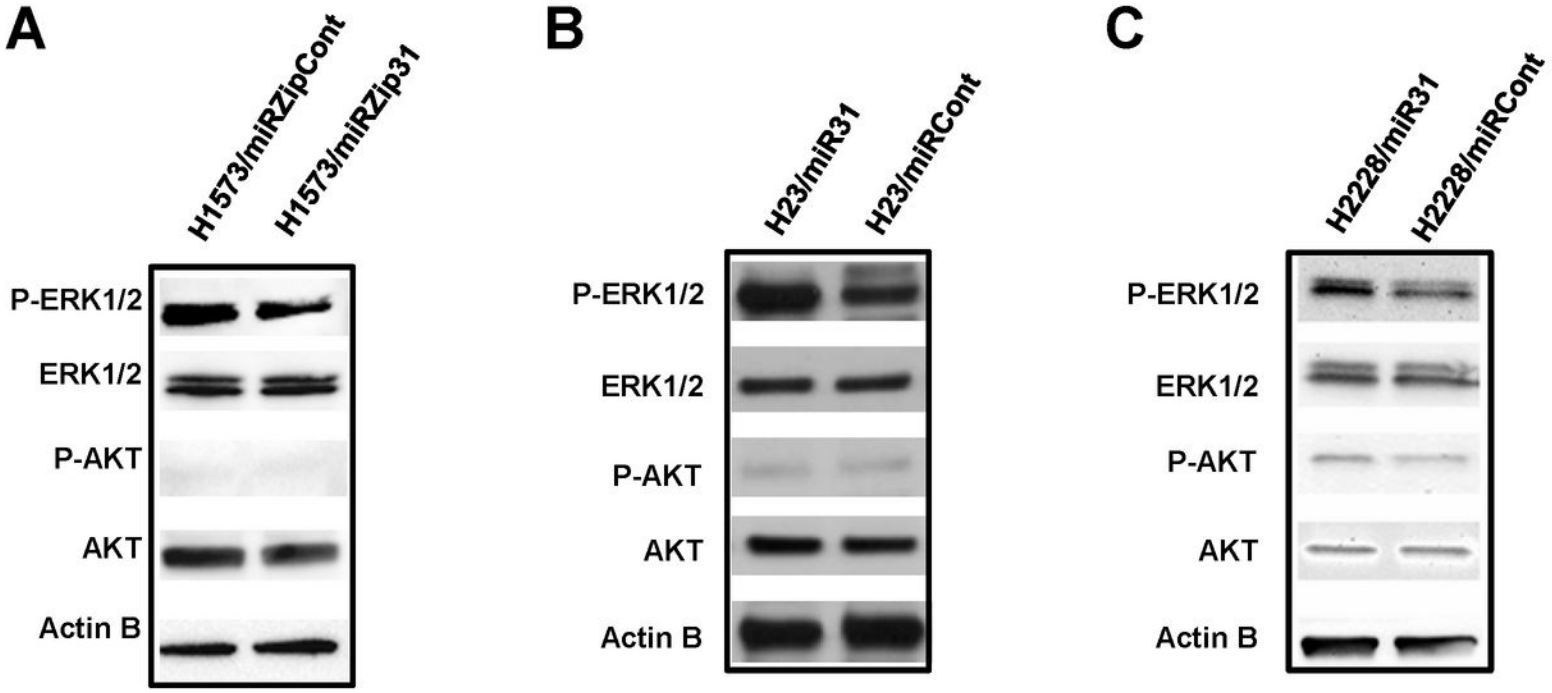

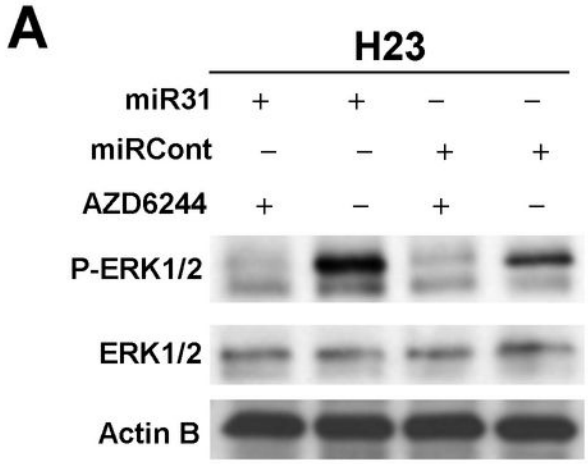

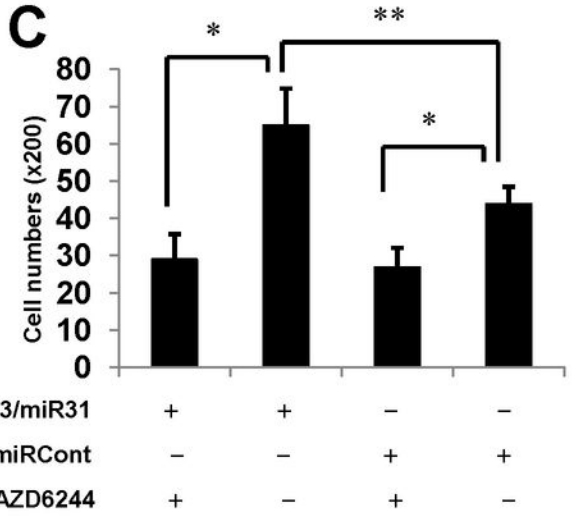

*<0.0005, **<0.005

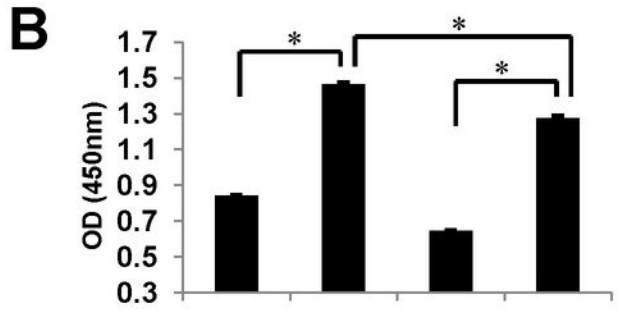

*<0.0005

AACR American Association for Cancer Research

Clinical Cancer Research

MicroRNA-31 predicts the presence of lymph node metastases and survival in lung adenocarcinoma patients

Wei Meng, Zhenqing Ye, Ri Cui, et al.

Clin Cancer Res Published OnlineFirst August 14, 2013.